ELSEVIER

Soil Dynamics and Earthquake Engineering 25 (2005) 795–809

SOIL DYNAMICS AND EARTHQUAKE ENGINEERING

www.elsevier.com/locate/soildyn

Seismic earth pressures on rigid and flexible retaining walls

P.N. Psarropoulos[a,*], G. Klonaris[b], G. Gazetas[a]

[a]School of Civil Engineering, National Technical University, Athens, Greece
[b]Mueser Rutledge Consulting Engineers, New York, USA

Accepted 11 November 2004

Abstract

While limiting-equilibrium Mononobe–Okabe type solutions are still widely used in designing rigid gravity and flexible cantilever retaining walls against earthquakes, elasticity-based solutions have been given a new impetus following the analytical work of Veletsos and Younan [23]. The present paper develops a more general finite-element method of solution, the results of which are shown to be in agreement with the available analytical results for the distribution of dynamic earth pressures on rigid and flexible walls. The method is then employed to further investigate parametrically the effects of flexural wall rigidity and the rocking base compliance. Both homogeneous and inhomogeneous retained soil is considered, while a second soil layer is introduced as the foundation of the retaining system. The results confirm the approximate convergence between Mononobe–Okabe and elasticity-based solutions for structurally or rotationally flexible walls. At the same time they show the beneficial effect of soil inhomogeneity and that wave propagation in the underlying foundation layer may have an effect that cannot be simply accounted for with an appropriate rocking spring at the base.

Keywords: Retaining walls; Dynamic earth pressures; Finite-element analysis; Layered soil; Mononobe–Okabe

1. Introduction

For many decades, the seismic analysis of retaining walls has been based on the simple extension of Coulomb's limit-equilibrium analysis, which has become widely known as the Mononobe–Okabe method ([14,11]). The method, modified and simplified by Seed and Whitman [19], has prevailed mainly due to its simplicity and the familiarity of engineers with the Coulomb method.

Experimental studies in the 1960s and 1970s using small-scale shaking table tests proved in many cases that the Mononobe–Okabe method was quite realistic, at least if the outward displacement of the wall (either due to translation, or rotation, or bending deformation) was large enough to cause the formation of a Coulomb-type sliding surface in the retained soil. A significant further development on the Mononobe–Okabe method has been its use by Richards and Elms [17] in determining permanent (inelastic) outward displacements using the Newmark sliding block concept [13].

However, in many real cases (basement walls, braced walls, bridge abutments, etc.) the kinematic constraints imposed on the retaining system would not lead to the development of limit-equilibrium conditions, and thereby increased dynamic earth pressures would be generated [7]. Elastic analytical solutions were first published by Scott [18], Wood [24], and Arias et al. [3]. The Wood solution referred to an absolutely rigid wall fixed at its base; the derived elastic dynamic earth pressures are more than two times higher than the pressures obtained with the limit-equilibrium methods. This fact, and the scarcity of spectacular failures of retaining walls during earthquakes, led to the widely-held impression that the elastic methods are over-conservative and inappropriate for practical use. This was the main reason for the nearly exclusive use of Mononobe–Okabe (and Seed–Whitman) method in engineering practice.

The two groups of methods mentioned above (elastic and limit-equilibrium) seem to cover the two extreme cases. The elastic methods regard the soil as a visco-elastic continuum, while limit-equilibrium methods assume rigid plastic behaviour. Efforts to bridge the gap between the above extremes have been reported by Whitman and his

* Corresponding author. Tel./fax: +1 30 210 894 5275.
E-mail address: prod@central.ntua.gr (P.N. Psarropoulos).

0267-7261/$ - see front matter © 2005 Elsevier Ltd. All rights reserved.
doi:10.1016/j.soildyn.2004.11.020

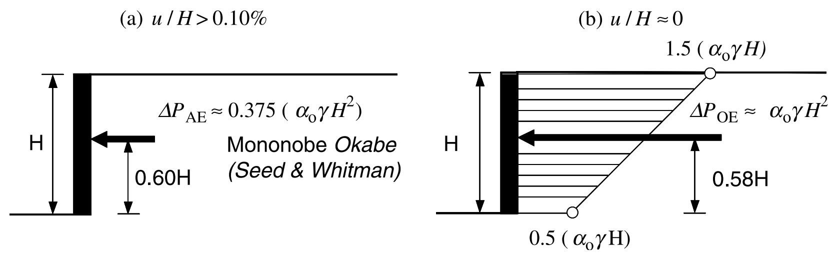

Fig. 1. Typical dynamic pressure distributions proposed in seismic bridge codes for seismic analysis of abutments. Situations (a) and (b) correspond to the two extreme cases: (a) of yielding wall supporting elasto-plastic soil in limit equilibrium, and (b) of undeformable and non-yielding wall supporting purely elastic soil. For intermediate size of wall displacements: $\Delta P = 0.75(\alpha_0 \gamma H^2)$.

co-workers ([1,2,12]). Their analyses combine wave propagation in a visco-elastic continuum with concentrated plastic deformation on a failure surface.

Based on the aforementioned categorization, many codes estimate the dynamic earth pressures according to the potential of the wall to deform. For example, the Greek Regulatory Guide E39/93 [16], referring to the seismic analysis of bridge abutments, proposes three different cases for the calculation of the dynamic earth pressures depending on the ratio between the displacement at the top of the wall u to its height H (see Fig. 1). As it is possible for the wall–soil system to develop material (or even geometric) non-linearities, it is difficult to distinguish the limits between the three cases. The main reason is that the displacement U cannot be predefined. It is obvious though, that the minimum dynamic earth pressures are predicted in the case of flexible walls ($u/H > 0.10\%$), while the dynamic pressures are almost 2.5 times higher in the case of perfectly rigid immovable walls ($u/H \approx 0$). For intermediate cases, the dynamic earth pressures are somewhere between the maximum and minimum value (see Ref. [15]).

It was not until recently that Veletsos and Younan [21–23] proved that the very high dynamic earth pressures of the elastic methods are attributed to the assumptions of rigid and fixed-based wall, which are an oversimplification of reality. To overcome this limitation, they developed an analytical solution that could account for the structural flexibility of the wall and/or the rotational compliance at its base; the latter was achieved through a rotational spring at the base of the wall. They discovered that the dynamic pressures depend profoundly on both the wall flexibility and the foundation rotational compliance, and that for realistic values of these factors the dynamic pressures are substantially lower than the pressures for a rigid, fixed-based wall. In fact, they found out that the dynamic pressures may reduce to the level of the Mononobe–Okabe solution if either the wall or the base flexibility is substantial.

However, these analytical solutions are based on the assumption of homogeneous retained soil, and there are reasons for someone to believe that the potential soil inhomogeneity may lead to significant changes in the magnitude and distribution of the dynamic earth pressures. Furthermore, as the presence of the foundation soil layers under the retained system is only crudely modelled through a rotational spring, these solutions do not account for the potential horizontal translation at the wall base, which in general may have both an elastic and an inelastic (sliding) component.

In the present paper, after a numerical verification of the analytical solution of Veletsos and Younan (utilising the finite-element method), the versatility of the finite-element method permits the treatment of some more realistic situations that are not amenable to analytical solution. So the modelling was extended to account for: (a) soil inhomogeneity of the retained soil, and (b) translational

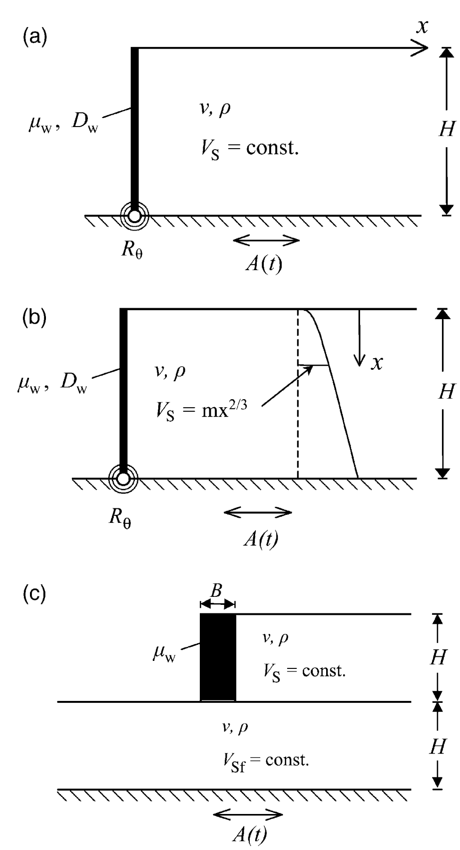

Fig. 2. The systems examined in this study: (a) flexible wall elastically restrained at its base, and retaining a homogeneous soil layer, (b) flexible wall elastically restrained at its base, and retaining an inhomogeneous soil layer, and (c) rigid gravity wall in a two-layer soil system.

flexibility of the wall foundation. Fig. 2 outlines the cases studied in this paper. Evidently:

- Case (a) coincides with the single-layer case studied in [23], where the retained soil is characterized by homogeneity.
- Case (b) models the same single-layer case, but the retained soil is inhomogeneous, with the shear modulus vanishing at the soil surface.
- Case (c) refers to a rigid wall founded on a soil stratum.

The results show that the inhomogeneity of the retained soil leads to reduced earth pressures near the top of the wall, especially in the case of very flexible walls, while the compliance of the foundation may not easily be modelled by a single rotational spring, due to wave propagation phenomena.

2. Flexible cantilever wall

2.1. Case A: homogeneous soil

Veletsos and Younan in 1997 [23] developed an analytical approach for evaluating the magnitude and distribution of the dynamic displacements, pressures, and forces induced by horizontal ground shaking in walls that are both flexible and elastically constrained against rotation at their base. The simplicity of their analytical tool permitted the assessment of the effects and relative importance of the factors involved.

In their model, the soil is considered to act as a uniform, infinitely extended visco-elastic stratum of height H. The properties of the soil are regarded constant, and defined by the density ρ, the shear modulus G, and Poisson's ratio ν. The material damping is presumed to be of the constant hysteretic type and is defined by the critical damping ratio ξ.

The layer is free at its upper surface, fixed on a rigid base, and it is retained by a vertical, flexible wall, elastically constrained against rotation at its base. The properties of the wall are described by its thickness t_{w}, mass per unit of surface area μ_{w}, modulus of elasticity E_{w}, Poisson's ratio ν, and critical damping ratio ξ_{w}. The stiffness of the rotational base constraint is denoted by R_{θ}.

The bases of the wall and the soil stratum are considered to be excited by a space-invariant horizontal motion, assuming an equivalent force-excited system.

The factors examined are the characteristics of the ground motion, the properties of the soil stratum, and the flexibilities of the wall and the rotational constraint at its base. Emphasis is given on the long-period—effectively static—harmonic excitations. The response for a dynamically excited system is then given as the product of the corresponding static response with an appropriate amplification (or de-amplification) factor.

The whole approach is based on the following simplifying assumptions:

- no de-bonding or relative slip is allowed to occur at the wall–soil interface.
- no vertical normal stresses develop anywhere in the medium, i.e. $\sigma_{\mathrm{y}}=0$, under the considered horizontal excitation.
- the horizontal variations of the vertical displacements are negligible.
- the wall is considered to be massless.

While the first assumption was made in order to obtain a simplified model, the other three assumptions were made to simplify the solution of the resulting equations that describe the behaviour of the model.

The main parameters that affect the response of the system are the relative flexibility of the wall and retained soil, defined by

$$d_{\mathrm{w}} = \frac{GH^3}{D_{\mathrm{w}}} \tag{1}$$

and the relative flexibility of the rotational base constraint and retained soil, defined by

$$d_{\theta} = \frac{GH^2}{R_{\theta}} \tag{2}$$

D_{w} in Eq. (1) denotes the flexural rigidity per unit of length of the wall:

$$D_{\mathrm{w}} = \frac{E_{\mathrm{w}} t_{\mathrm{w}}^3}{12(1-\nu_{\mathrm{w}}^2)} \tag{3}$$

What also affect the response are the characteristics of the input base motion. For a harmonic excitation the response is controlled by the frequency ratio ω/ω_1, where ω is the dominant cyclic frequency of the excitation, and ω_1 the fundamental cyclic frequency of the soil stratum.

2.1.1. Numerical modelling

This study focuses primarily on the numerical verification of the analytical results of Veletsos and Younan, using exactly the same model for the wall–soil system. The purpose was to validate the assumptions of the analytical solution and to define the range of its applicability.

Presuming plane-strain conditions, the numerical analysis was two-dimensional, and was performed using the commercial finite-element package ABAQUS [8]. The finite-element model of the wall–soil system examined is shown in Fig. 3.

By trial analyses it was established that the magnitude of the wall pressures is proportional to the wall height, which was also noted in the analytical solution. Taking that into account, all the analyses were performed considering an 8 m-high wall. The wall itself was discretized by beam elements, of unit longitudinal dimension

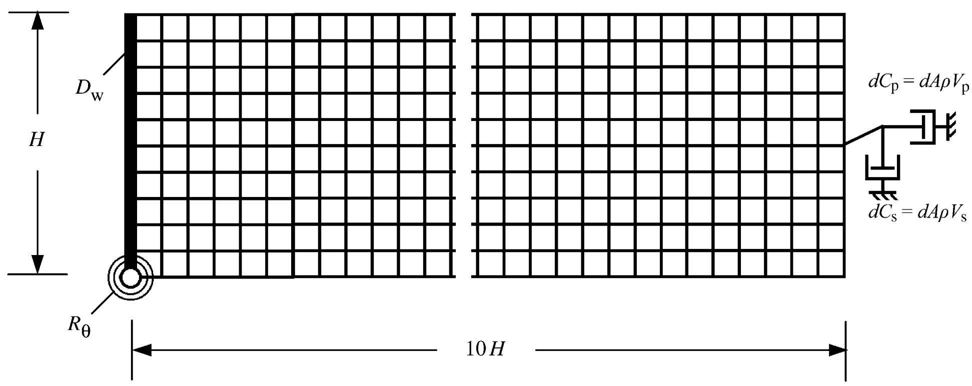

Fig. 3. The finite-element discretization of the examined single-layer systems. The base of the model is fixed, while absorbing boundaries have been placed on the right-hand artificial boundary.

and thickness $t_w = 0.20$ m. Given the value of d_w, the modulus of elasticity of the wall E_w derives from Eqs. (1) and (3), while the Poisson's ratio is 0.2. The wall mass per unit of surface area μ_w is presumed to be 2.5 t/m^2. It is reminded that Veletsos and Younan had regarded the wall as massless. At the base of the wall a rotational constraint was placed, the stiffness of which is denoted by R_θ. Eq. (2) relates d_θ with R_θ.

The discretization of the retained soil is made by two-dimensional, four-noded quadrilateral, plane-strain elements. Since, the finite-element grid cannot extend infinitely, there is a need for using absorbing boundaries in order to simulate the radiation of energy. The latter is achieved using horizontal and vertical viscous dashpots, which absorb the radiated energy from the P and S waves, respectively. The efficiency of the viscous dashpots is in general quite acceptable, but as it depends strongly on the angle of incidence of the impinging wave the dashpots were placed $10H$ away from the wall to improve the accuracy of the simulation (see Fig. 3). The soil is presumed to act as a visco-elastic material. Trial analyses indicated that the wall pressures are not directly affected by the shear modulus value of the retained soil. The shear modulus value affects the wall pressures indirectly via the relative flexibility factors (d_w and d_θ), and the eigenfrequency of the soil stratum. Therefore, for the analyses presented in this section the density ρ and the shear wave velocity V_S are assumed to be 1.8 t/m^3 and 100 m/s, respectively. Furthermore, the Poisson's ratio ν is presumed to be 1/3, while critical damping ratio ξ is 5%.

Regarding the wall–soil interface, although the option of de-bonding and relative sliding was available in ABAQUS [8], the assumption of complete bonding—made by Veletsos and Younan—was also adopted to permit a comparative study.

The excitation was introduced by a prescribed acceleration time history on the nodes of the wall and the soil-stratum bases. The case of harmonic excitation was examined:

$$A(t) = A_0 \sin(\omega t), \quad \text{where} \quad A_0 = 1 \text{ m/s}^2 \tag{4}$$

The duration chosen for all numerical analyses was such that steady state conditions were always reached.

2.1.2. Problem parameters

The dimensionless parameters of the problem examined are three: the relative flexibility factors d_w and d_θ, and the ratio of the cyclic frequency of the excitation to the fundamental cyclic eigenfrequency of the soil layer ω/ω_1. The values of parameters were the following:

$d_w = 0$ (rigid wall), 1, 5, and 40
$d_\theta = 0$ (fixed against rotation), 0.5, 1, and 5
$\omega/\omega_1 = 1/6$ (practically static case), 1 (resonance), and 3 (high-frequency motion).

2.1.3. Quasi-static response

Initially, the response of the system under nearly static excitation is examined. Practically, that is achieved by a harmonic ground motion with frequency very low compared to the fundamental eigenfrequency of the soil stratum ($\omega/\omega_1 = 1/6$). For this value of frequency ratio, all the possible combinations of the parameters d_w and d_θ are considered.

The heightwise distributions of the statically induced wall pressures $\sigma_{st} = \sigma_{st}(\eta)$ for systems with different values of the relative flexibility factors d_w and d_θ are shown in Fig. 4. The values of the pressures, plotted on the horizontal graph axis, are normalized with respect to $\alpha_0\gamma H$, where α_0 is the maximum acceleration at the base expressed in g, γ is the unit weight of the retained soil, and H is the height of the wall. On the vertical graph axis, the y-coordinate of the corresponding point along the inner side of the wall, normalized with respect to the wall's height is plotted ($\eta = y/H$). The pressures are considered positive when they induce compression on the wall. Note that all the results presented in this paper refer to the incremental (dynamic) loads due to horizontal shaking.

It is observed that, for relatively high values of d_w and d_θ, negative pressures (i.e. tensile stresses) are developed near

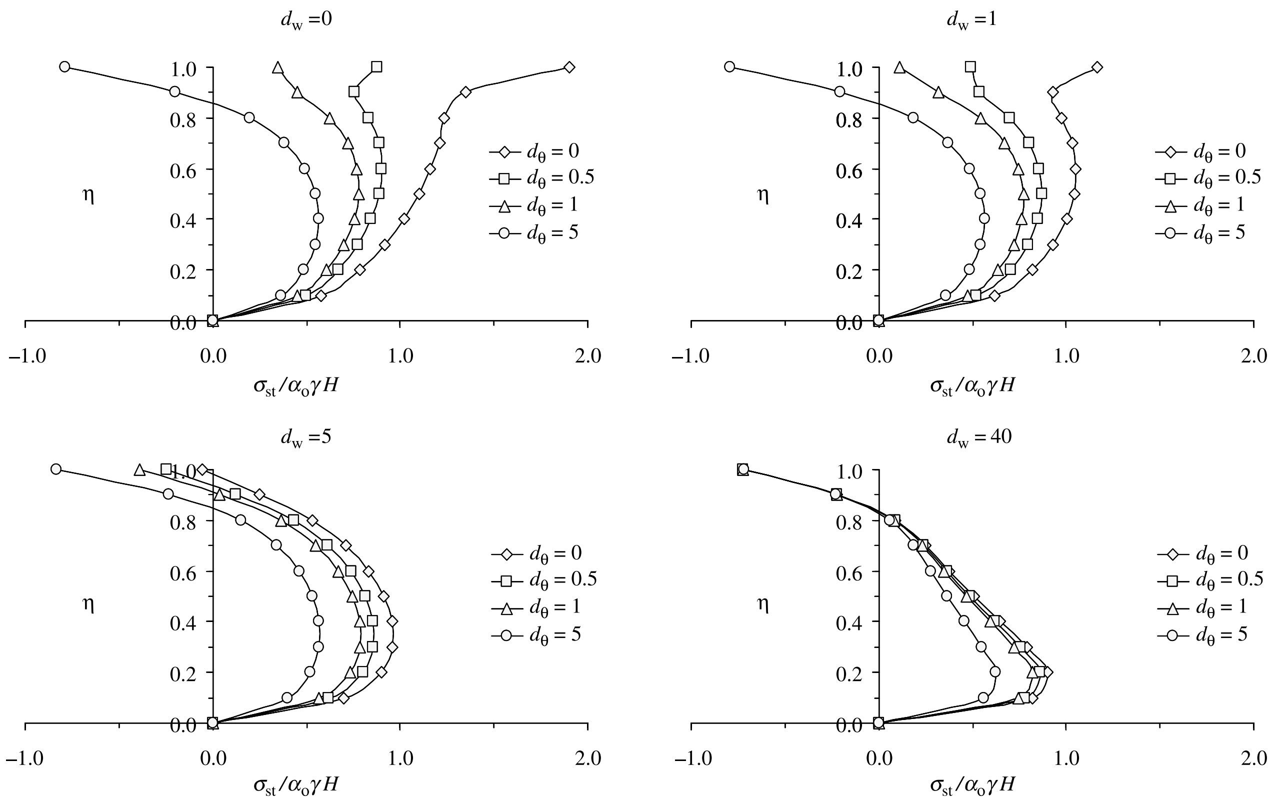

Fig. 4. Earth-pressure distribution of a quasi-statically excited retaining system with varying relative flexibility, d_θ , of the base rotational spring for different values of relative wall flexibility, d_w.

the top of the wall. In case that the absolute value of these stresses exceeds the initial geostatic stresses, de-bonding will occur, making the initial assumption unrealistic. Therefore, it was decided—and it is suggested—to ignore these tensile stresses when integrating the wall pressures in order to calculate the resultant force and the corresponding overturning moment.

Notice that, as the values of the relative flexibility factors increase, the wall pressures decrease. It is reminded that the increase of d_w and d_θ implies increase of the flexibility of the wall and its base. Apart from the pressure decrease—which affects the resultant force on the wall (see Fig. 5(a))—the increased values of d_w and d_θ have an additional beneficial effect. For relatively rigid systems there is a sinusoidal-like increase of the pressures from the base to the top of the wall, while flexible systems tend to exhibit a triangular-like distribution. As a consequence, the corresponding overturning moment of flexible walls (see Fig. 5(b)) is reduced due to the effective height decrease (see Fig. 6).

It is interesting to compare (Fig. 5) the resultant forces and overturning moments, with the ones proposed by Seed and Whitman [19], which are based on Mononobe–Okabe method and the accumulated experimental experience:

$$\Delta P_E = 0.375\alpha_0\gamma H^2 \tag{5}$$

$$\Delta M_E = (0.6H)\Delta P_E \tag{6}$$

According to Figs. 5 and 6, it is evident that:

- in the case of very flexible walls (high values of d_w) the resultant force and the corresponding overturning moment are quite insensitive to the variation of the base flexibility (values of d_θ).
- the results of the proposed model are in agreement with the ones derived by [19], as far as base shear is concerned, when the base flexibility is relatively high ($d_\theta = 5$).
- the above remark is not valid for the case of the overturning moment, mainly because of the conservative estimation of the effective height made by Seed and Whitman. Note that in Fig. 6 the upper limit and the lower limit of the effective height coincide with the value proposed by Seed and Whitman ($0.6H$) and Mononobe–Okabe method ($0.33H$), respectively.

Of special interest is the horizontal distribution of the normal and shear stresses in the retained soil, shown in Fig. 7. The results presented correspond to the stress conditions along a straight horizontal line in the middle of the soil layer for the two extreme cases examined—$d_w = 0$, $d_\theta = 0$ and $d_w = 40$, $d_\theta = 5$. The increase in the flexibility of

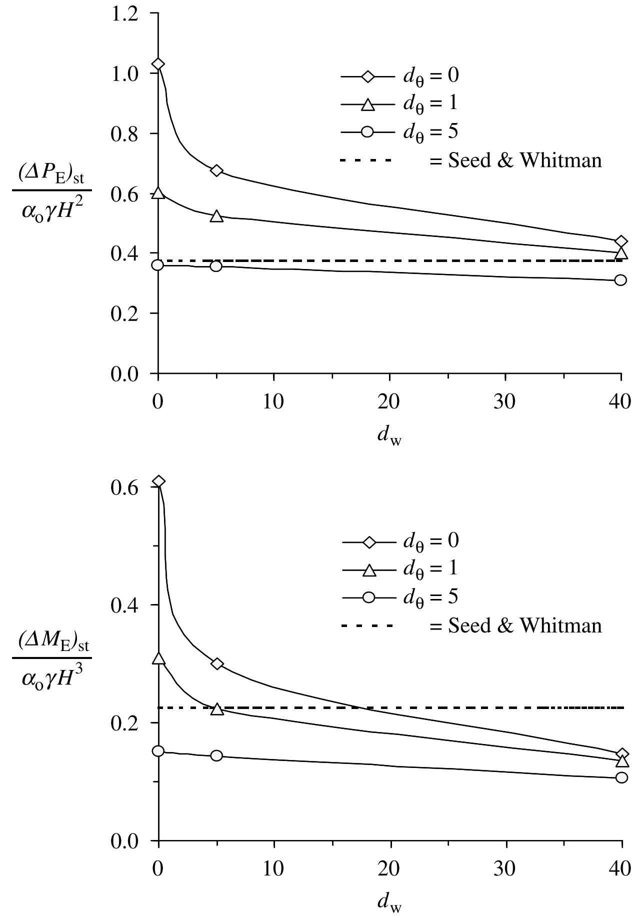

Fig. 5. Normalized values of resultant dynamic horizontal force $(\Delta P_E)_{st}$ and resultant dynamic overturning moment $(\Delta M_E)_{st}$ on a pseudo-statically excited wall, with different wall and base flexibilities (d_w and d_θ), compared with the values proposed by Seed and Whitman in [19].

the system decreases the percentage of the developed inertial forces transferred to the retaining wall through the soil extensional stiffness to those transferred to the layer base through its shear stiffness. This was rather expected

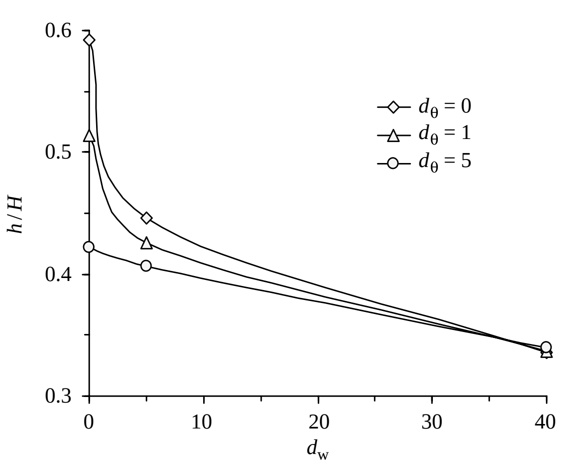

Fig. 6. Normalized height h from the base of the resultant force on the wall (called 'effective' height by Veletsos and Younan [23]) for quasi-statically excited systems, having different wall and base flexibilities (d_w and d_θ).

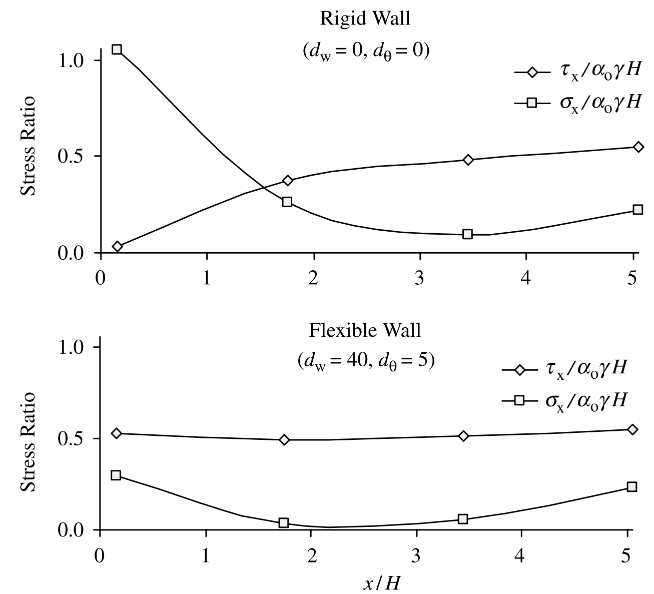

Fig. 7. Distribution of horizontal normal stresses (σ_x) and shear stresses (τ_{xy}) developed along a horizontal line at mid-depth in the retained soil for pseudo-static excitation for rigid and flexible wall.

and explains the variation of the magnitude of the wall pressures shown in Fig. 4.

Knowing the distribution of normal and shear stresses developed in the retained soil, it is feasible to assess the validity of the assumption regarding no relative sliding along the wall–soil interface. The friction angle between the wall and the retained soil can be taken as $\delta \approx \varphi/2$, where φ is the internal friction angle of the soil. For typical values of φ (30–35°) sliding does not occur when the following condition is satisfied:

$$\tau_{xy}/\sigma_x \leq \tan \delta \approx 0.3 \tag{7}$$

Obviously, Eq. (7) cannot be used as-is to compute the exact value of the stress ratio necessary to cause slipping at the wall–soil interface, because the initial state of stress is not known. Nevertheless, ratios $\tau_{xy}/\sigma_x > 1.0$ (the case of flexible walls, Fig. 8) indicate that no matter what the static

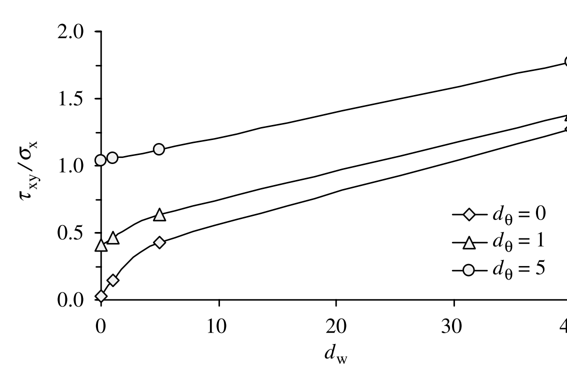

Fig. 8. Comparison of shear and normal stresses at the wall–soil interface in the case of statically excited systems with different wall and base flexibilities (d_w and d_θ).

state of stress is before shaking, slippage will definitely occur.

2.1.4. Analytical verification of the quasi-static response

In this section, a comparison between the analytical solution given by Veletsos and Younan and the numerical results presented in the previous section is performed. The distributions of seismic wall pressures in the case of statically excited systems and for different wall and base flexibilities (d_w and d_θ) are shown in Fig. 9. The analytical solution is represented by continuous line, while dots have been used for the representation of the numerical results. In general, the two solutions are in good agreement for every combination of flexibilities, while the only discrepancy observed is near the top of the wall, especially in the case of systems with low flexibility. The distributions resulting from the numerical solution exhibit a concave deviation while approaching the free surface. This phenomenon has also been observed by other researchers (see Ref. [24]) and characterizes numerical solutions. This comparison establishes, at least to a point, the validity of the assumptions made in the analytical solution, regarding the vertical normal stresses and the mass of the wall.

Though the wall pressures predicted by the analytical formulation and the numerical model seem to be in agreement, the same is not observed for the base shear and the overturning moment, as shown in Fig. 10. It is reminded that in the post-processing of the numerical results, tensile stresses have been regarded as unrealistic, and therefore, ignored. As a consequence, the 'produced' results (base shear and overturning moment) tend to be in agreement only in the case of rigid systems, where no tensile stresses are developed, while, on the other hand, the analytical solution underestimates both the base shear and the overturning moment in the case of flexible systems. It is worth mentioning that the discrepancies observed are more substantial for the overturning moment, and may even lead to a 50% increase of the corresponding analytical ones. That fact seems quite logical considering the double effect of the tensile stresses: (a) the reduction of the base shear, and (b) the reduction of the corresponding effective height.

2.1.5. Harmonic response

Typical values for the fundamental frequency of the soil stratum may be between 2 and 15 Hz, while the dominant frequency of a seismically induced excitation ranges from 2 to 5 Hz. Thus, the case of statically excited systems examined before may be encountered in practice, apart from its theoretical interest. Nevertheless, it is obvious that resonance phenomena are also possible. For all possible combinations of d_w and d_θ, two values of the frequency ratio are examined:

$\omega/\omega_1 = 1$ (resonance)
$\omega/\omega_1 = 3$ (high-frequency motion).

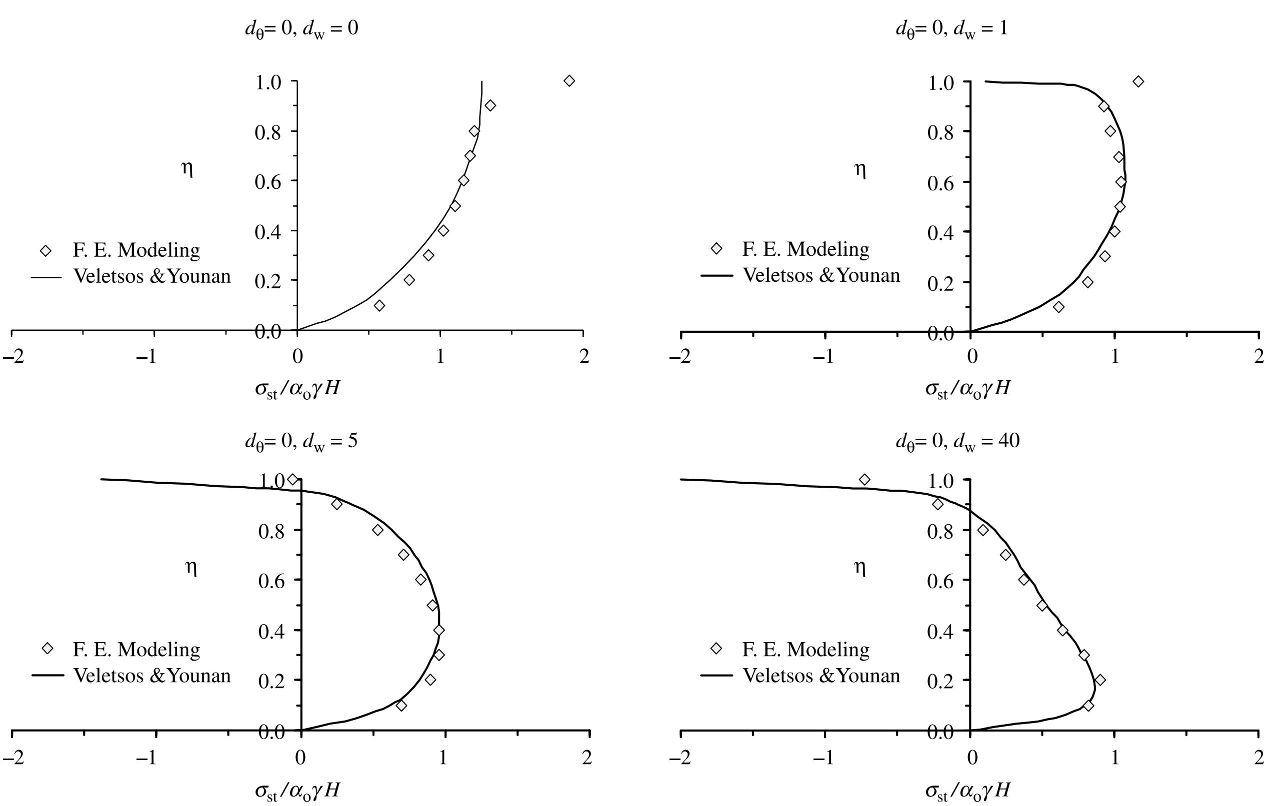

Fig. 9. Comparison of the distributions of the earth pressures on the wall computed with our numerical method and those computed analytically by Veletsos and Younan in [23]. Quasi-statically excited fixed-base walls ($d_\theta = 0$) with different wall flexibilities d_w.

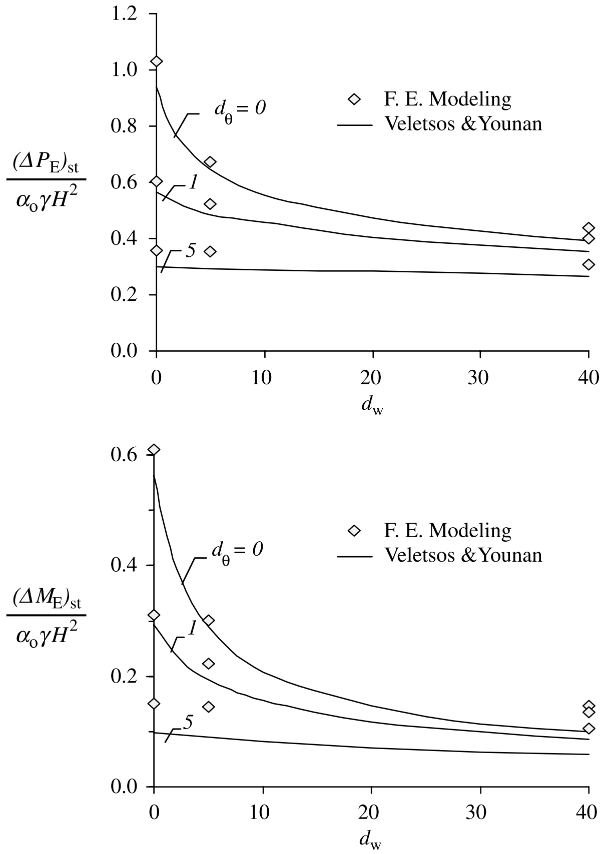

Fig. 10. Comparison between the normalized values of base shear $(\Delta P_E)_{st}$ and overturning moment $(\Delta M_E)_{st}$ from the analytical formulation (continuous line) of Veletsos and Younan in [23] and those of the numerical simulation (dots) of our study. Quasi-statically excited systems with different wall and base flexibilities (d_w and d_θ).

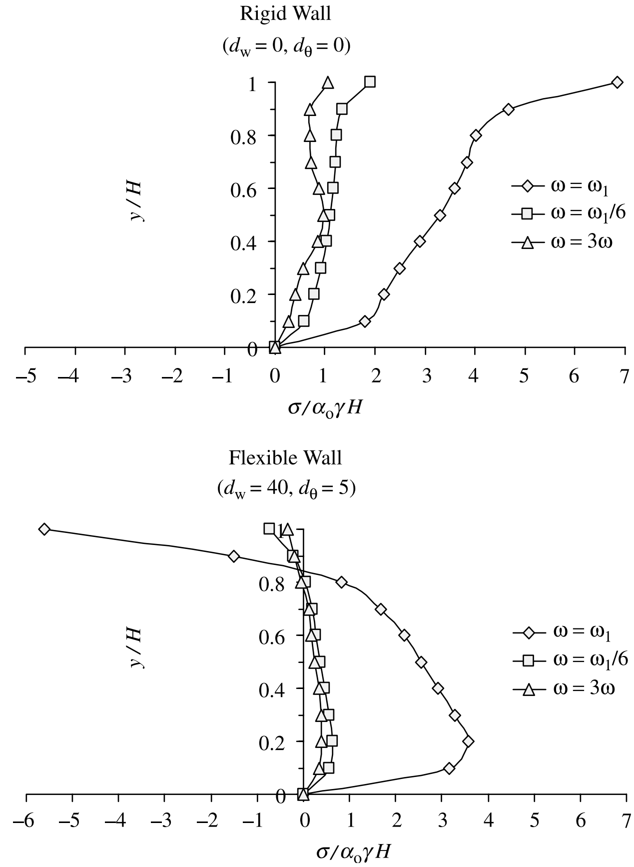

Fig. 11. Steady-state earth pressure distribution for three excitation frequencies: $\omega = \omega_1$, $\omega = \omega_1/6$, and $\omega = 3\omega_1$, where ω_1 is the fundamental frequency of the wall–layer system.

As previously mentioned the analyses were performed assuming constant height and constant shear wave velocity of the soil stratum. Therefore, ω_1 was constant for all analyses, and the variability in ω/ω_1 was undertaken by varying ω.

Fig. 11 shows the effect of the excitation frequency on the magnitude and the distribution of the wall pressures only for the extreme cases of flexibility examined: rigid wall ($d_w = 0$, $d_\theta = 0$), and very flexible wall ($d_w = 40$, $d_\theta = 5$).

Comparing the wall pressure distribution in the case of resonance ($\omega/\omega_1 = 1$) with that of the corresponding static excitation, the following conclusions may be drawn:

- for every combination of d_w and d_θ the pressures are increased in the case of soil resonance.
- the amount of increase is highly depended on the flexibility of the wall and its base. For low values of flexibility the dynamic amplification factor is about 3, while for higher values the amplification factor may be of the order of 7.
- the shape of the heightwise pressure distribution is not changed substantially, as the increase takes place uniformly.

In the case that $\omega/\omega_1 = 3$, a similar comparison leads to the following conclusions:

- this case is 'beneficial' for the wall itself, since the pressures are lower for every combination of flexibility.
- the amount of decrease is practically independent on the values of d_w and d_θ.
- the shape of the heightwise pressure distribution is different than the corresponding static, mainly due to the contribution of higher modes of vibration.

The above qualitative conclusions are expressed quantitatively in Fig. 12, where the maximum amplification factor for the resultant force (A_Q) and the corresponding overturning moment (A_M) are shown.

The increase of the amplification factor that is observed in Fig. 12 can be explained by the distribution of horizontal maximum acceleration in the backfill. The acceleration was recorded along two horizontal levels of height H and $H/2$ with respect to the base level. The results are plotted in Fig. 13, normalized to the maximum ground base acceleration, so as to express the amplification in the retained soil layer. It is evident that in the case of rigid and fixed wall (Fig. 13(a)) the motion in the vicinity of the wall is

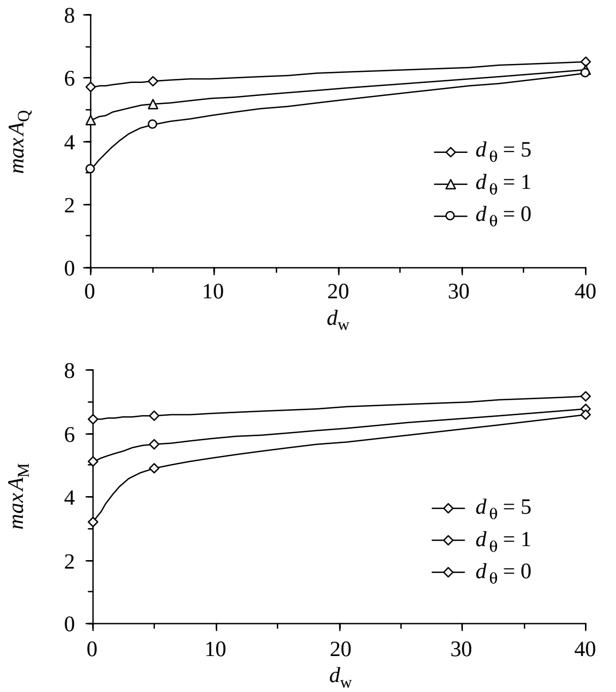

Fig. 12. Maximum values of the dynamic amplification factors A_Q and A_M for the resultant horizontal force and the resultant overturning moment, respectively, in case of a harmonically excited system with different wall and base flexibilities (d_w and d_θ).

practically induced by the wall itself, therefore, no amplification is observed. On the other hand, flexible systems (Fig. 13(b)) permit shear deformation, and consequently, higher levels of acceleration. In all cases, the amplification factor is maximized at a distance of about $3H$ from the wall. Like in the case of static loading (see Fig. 7), at that distance one-dimensional conditions are present, so

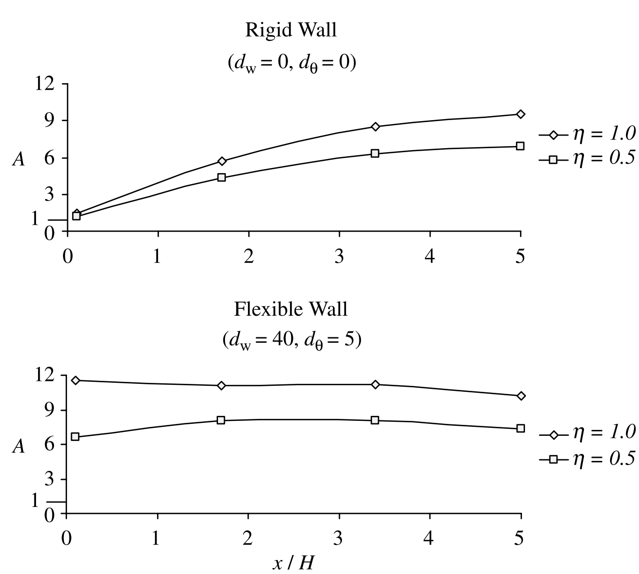

Fig. 13. Soil amplification of steady-state acceleration at resonance ($\omega = \omega_1$), along the surface ($\eta = 1$) and the mid-depth ($\eta = 0.5$) of the retained soil.

the expected maximum amplification factor for a soil layer with critical damping ratio ξ (see Roesset [25] and Kramer [26]) is given by:

$$A = \frac{1}{\sqrt{\cos^2\left(\frac{\pi}{2} + n\pi\right) + \left(\xi\left(\frac{\pi}{2} + n\pi\right)\right)^2}} = \frac{2}{\pi\xi}\frac{1}{2n+1} \qquad (8)$$

which for $n = 0$ (first mode) and $\xi = 5\%$ leads to $A \approx 12.5$.

This value is very close to that predicted by the numerical model, a fact that is indicative of the realistic simulation of the problem and its boundary conditions.

It is obvious that the assumption of uniform acceleration field in the retained soil, adopted by the limit-state methods, is not realistic for the case of dynamic excitation. Ignoring the amplification phenomena will likely lead to underestimation of the seismically induced wall pressures.

Nevertheless, such high levels of amplification would not occur in the case of a transient excitation. According to Veletsos and Younan [23], who examined analytically the transient response of the system under the 1940 El Centro excitation, the dynamic amplification factors range between 1.5 and 2 for total wall force, while the effective wall height seems rather insensitive to the ground motion. It is believed, however, that in cases of excitations characterized by narrow spectra with dominant frequencies (or periods) close to the fundamental eigenfrequency of the soil stratum, the amplification may be substantially higher, perhaps even approaching the values of harmonic loading at resonance.

2.2. Case B: inhomogeneous soil

In the previous sections, the properties of the retained soil were presumed constant. In reality, the soil shear modulus is likely to increase with depth. Such a inhomogeneity reflects in a very simple way, not only the unavoidably-reduced stiffness under the small confining pressures prevailing near the top, but two more strong-shaking effects:

(a) the softening of the soil due to large shearing deformations, and
(b) the non-linear wall–soil interface behaviour, including separation and slippage.

Note that this feature is too complicated to be incorporated in analytical formulations. Veletsos and Younan have examined analytically the inhomogeneity with depth, regarding a rigid wall elastically constrained against rotation at its base. To simplify, the equations of motion a specific parabolic variation of the shear modulus was used. The extension of the analytical solution to include the flexibility of the wall and/or additional variations of the shear modulus seems to be difficult. Here lies the greatest advantage of the finite-element method, which can cope boundlessly at least with the aforementioned features.

The response of statically excited wall–soil systems is examined, taking into account apart from the rotational flexibility, the flexibility of the wall, considering the following expression of the variation of the shear wave velocity (see Ref. [20]):

$$V_S = m(H - y)^{2/3} \tag{9}$$

where m is a parameter chosen so as the mean shear wave velocity V_S to be 100 m/s, and to permit the comparison with the results presented in the previous sections.

The finite-element model that was used, was the same with the one described in the previous sections (see Fig. 3), subjected to the necessary modifications regarding the varying soil properties. The values of the relative flexibility factors d_w and d_θ are given by

$$d_w = \frac{\bar{G}H^3}{D_w} \tag{10}$$

$$d_\theta = \frac{\bar{G}H^2}{R_\theta} \tag{11}$$

where $\overline{G}$ is the mean value of the shear modulus.

For the variation of the shear wave velocity considered here, the fundamental cyclic frequency of the retained soil layer can be proven (see Ref. [20]) to be

$$\omega_1 = \frac{\pi}{3}\frac{m}{H^{1/3}} \tag{12}$$

In order to study, the static response of the system, a harmonic excitation with cyclic frequency $\omega = \omega_1/6$ was considered.

The heightwise distribution of the statically induced wall pressures are shown in Fig. 14 for systems with different wall and base flexibilities. It is observed that, due to the nullification of the soil shear modulus at the surface, the pressures developed near the top converge to the same value for every combination of d_w and d_θ. Therefore, no tensile stresses are present, making the assumption of complete bonding more realistic. In Fig. 15, a comparison between the homogeneous and the inhomogeneous soil is shown for the case of a rigid fixed-base wall and a very flexible fixed-base wall.

In Fig. 16, the normalized values of the resultant force and the corresponding overturning moment for statically excited systems and for different flexibilities are presented. It is obvious that the values in the case of inhomogeneous soil are substantially lower compared to those of homogeneous soil and the values proposed in [19].

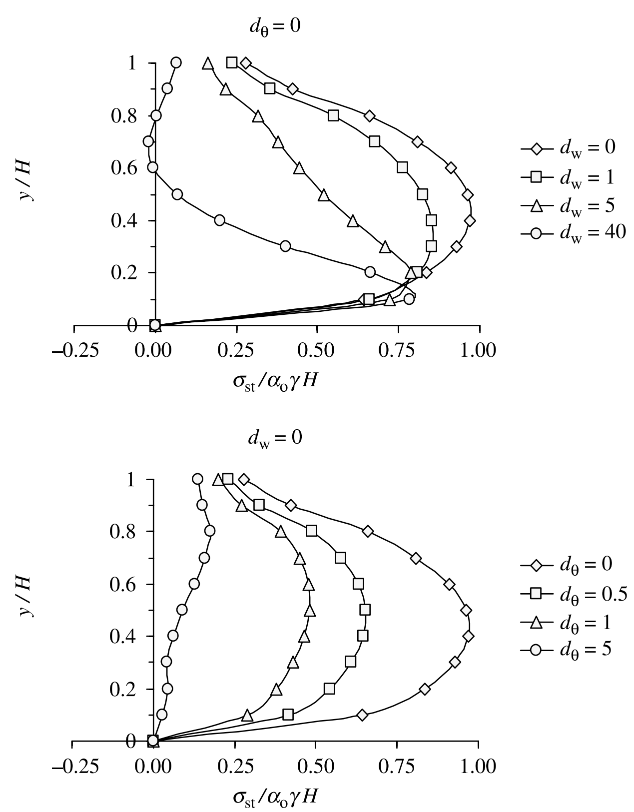

Fig. 14. Earth pressure distributions for statically excited walls retaining inhomogeneous soil, with different wall and base flexibilities (d_w and d_θ).

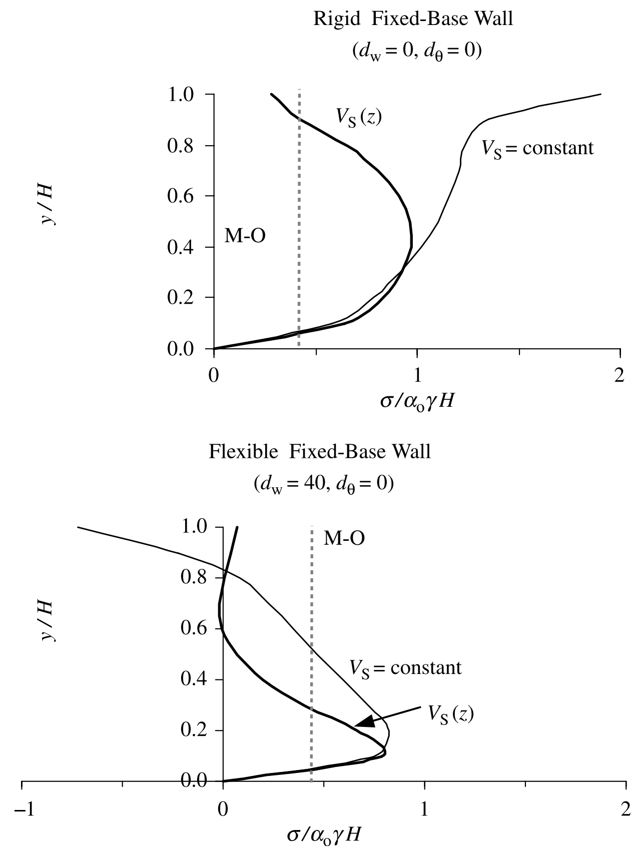

Fig. 15. Effect of soil inhomogeneity on the elastic dynamic earth-pressure distribution for a rigid fixed-base wall (d_w=0, d_θ=0) and for a flexible fixed-base wall (d_w=40, d_θ=0). Comparison with the corresponding curves for the homogeneous soil from Fig. 4.

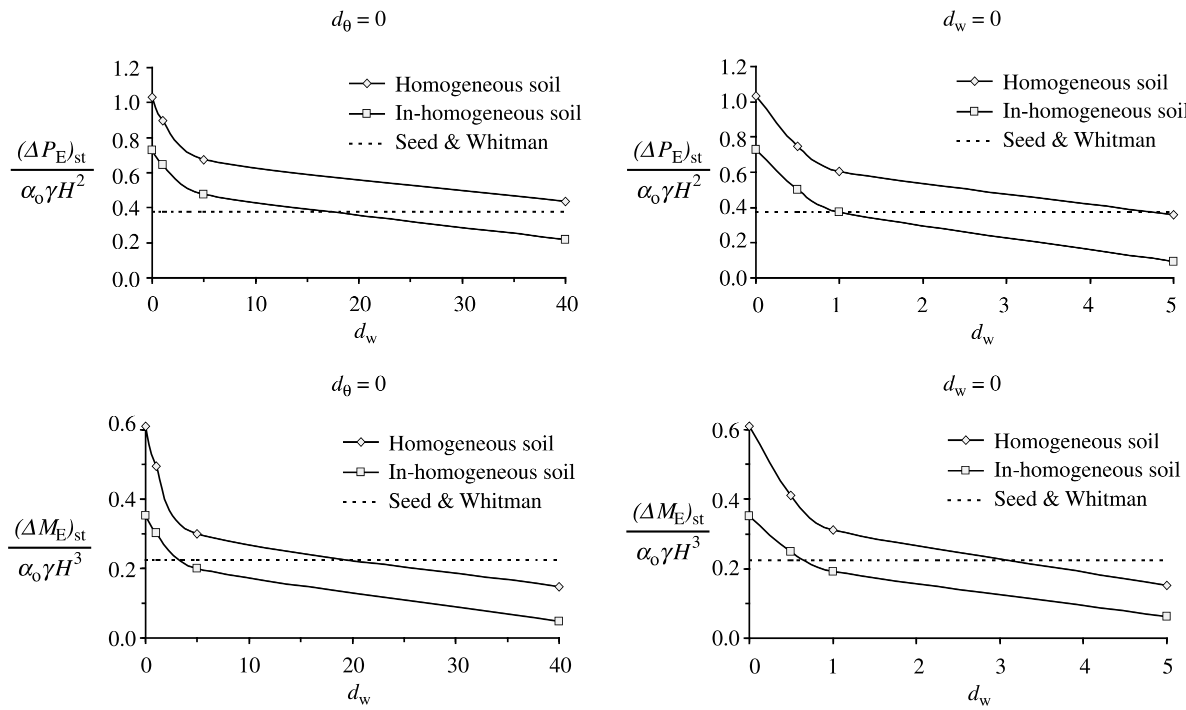

Fig. 16. Normalized values of resultant force and the overturning moment for statically excited wall, with different wall and base flexibilities (d_w and d_θ), for homogeneous and inhomogeneous soil, compared to the values proposed by Seed and Whitman in [19].

3. Two-layers system

In the aforementioned single-layer models the rotational stiffness of the wall foundation is simulated by a rotational elastic constraint at the base of the wall. It is evident that in this way, while the potential rotation of the wall is taken into account, horizontal translation is not allowed, thus reducing by one the degrees of freedom of the system. That simplification is expected to have a substantial effect on the response of the retaining structure. In this part of the study, in order to assess this effect, a more realistic model is examined, in which wall and the retained soil overlie a linearly visco-elastic soil layer. As the aim in this section is to evaluate the role of the wall foundation, only rigid gravity walls are examined ($d_w = 0$).

In the analytical system, the rotational stiffness of the wall foundation was expressed by a dimensionless relative flexibility factor, given by Eq. (2).

By substituting the rotational constraint by an equivalent soil layer underlying the wall and the retained soil, the number of the problem parameters increase substantially, since R_θ can be expressed by the relation proposed by [5,6]:

$$R_\theta = K_r \cong \frac{\pi G_f B^2}{8(1-\nu_f)}\left(1 + \frac{1}{10}\frac{B}{H_f}\right) \quad (13)$$

Relation (13) applies for the case of a strip footing of width B, resting on a soil layer which has thickness H_f, shear modulus G_f, and Poisson's ratio ν_f. Furthermore, by this replacement, the stiffness of the horizontal (transverse) translation K_h is taken into account, implying an additional degree of freedom in the system:

$$K_h \cong \frac{2.1 G_f}{2-\nu_f}\left(1 + \frac{B}{H_f}\right) \quad (14)$$

Let us consider two gravity walls of the same height H, different base width B, that retain soil layers with identical properties, and rest on soil layers of the same thickness H_f, but of different shear modulus G_f (so that the values of the rotational stiffness R_θ are equal for the two cases). The simple model with the rotational constraint at the base of the wall, hereafter referred to as *spring model*, suggests (for the same excitation) that the two systems have the same response, since they are characterized by common relative flexibility factor d_θ.

In reality, the two systems will respond differently, for the two following reasons:

- the values of translational stiffness K_h will defer, as is evident by Eq. (14).
- the existence of the underlying soil layer affects the fundamental frequency of the system, and therefore, the ratio ω/ω_1 is different in the two cases.

As it was established by the model proposed in [23], and verified in the previous sections, the response of a wall–soil system depends mainly on the flexibility of the system and the ratio ω/ω_1. Thus, a change in K_h and/or ω will reflect substantially on the system response.

It is worth mentioning that Eqs. (13) and (14) express static stiffness, and therefore, are 'accurate' for statically excited systems ($\omega/\omega_1 \to 0$). In the case of dynamic excitations the problem becomes even more complicated.

3.1.1. Numerical model

The wall–soil system considered consists of a gravity wall, which is founded on a horizontally infinite layer of visco-elastic soil material, bonded to a rigid base, and retains a semi-infinite layer of visco-elastic soil material free at its upper surface. Like in the single-layer models, we presume plane-strain conditions, the numerical analysis is two-dimensional, and it is performed using ABAQUS [8]. The model of the wall–soil system examined and the corresponding finite-element mesh are both shown in Fig. 17.

The case examined refers to a wall of height H, overlying a soil layer of the same height. The parameters considered are the following:

- the base width B to the wall height H ratio (B/H);
- the relative flexibility factor d_θ;
- the ratio of the dominant excitation cyclic frequency ω to the fundamental cyclic frequency ω_1 of the two-layered profile.

The discretization of the whole system was performed by two-dimensional, plane-strain, quadrilateral four-noded finite elements, while the finite-element mesh is truncated by the use of viscous dashpots (see Fig. 17).

The properties of the retained and the foundation soil are also shown in Fig. 17. The shear wave velocity V_{Sf}, of the foundation soil is determined by Eqs. (2) and (3), for a given value of d_θ. The critical damping ratio ξ, was presumed to be 5% for both soil layers. The wall was regarded as rigid with mass per unit of surface area $\mu_{\mathrm{w}} = 2.5\ \mathrm{t/m^2}$.

Regarding the interfaces between the wall and either the retained or the foundation soil, it was considered that neither de-bonding, nor relative slip occurs.

The excitation was introduced by a prescribed acceleration time history on the nodes of the foundation soil-stratum base. The case of harmonic excitation was examined:

$$A(t) = A_0 \sin(\omega t), \quad \text{where } A_0 = 1\ \mathrm{m/s^2} \tag{15}$$

Two values of the excitation cyclic frequency ω were examined: $\omega = \omega_1/6$ (almost static), and $\omega = \omega_1$ (resonance), where ω_1 is the fundamental cyclic frequency of the two-layers profile.

The value of ω_1 was computed by the Rayleigh algorithm (see Ref. [4]), which, in the case of two soil layers with

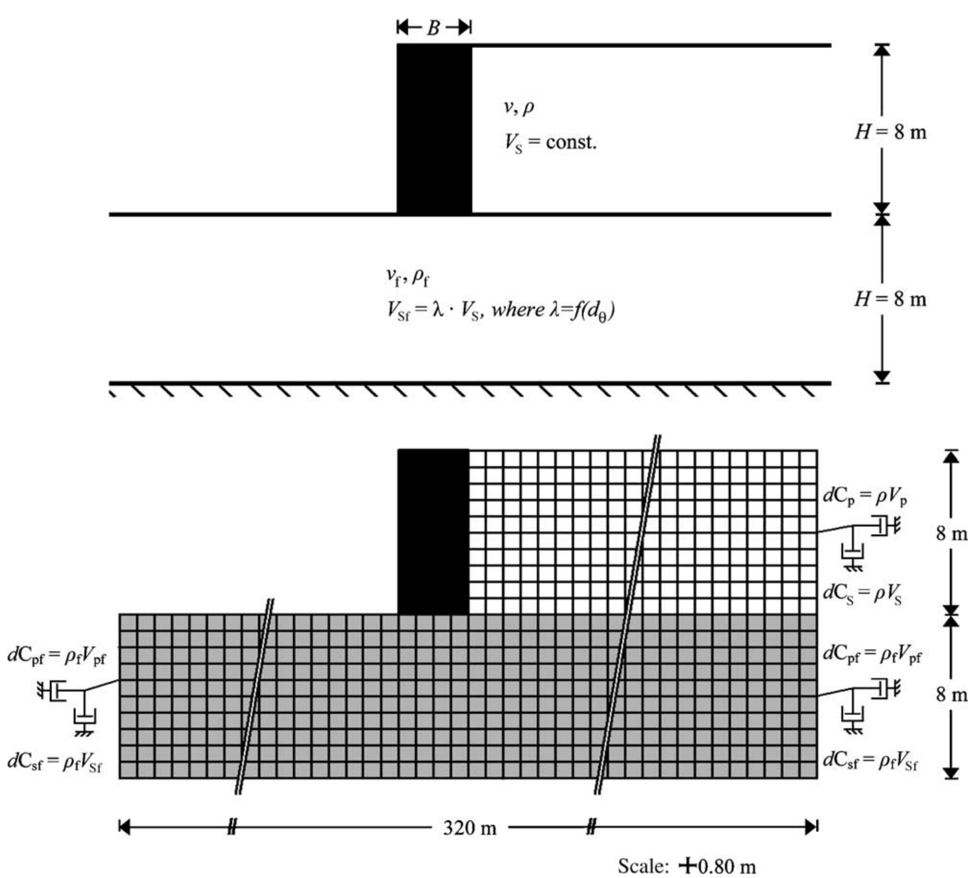

Fig. 17. The system under consideration (gravity wall founded on soil layer) and the corresponding finite-element model.

equal thickness H, has the form:

$$\omega_1^2 = \frac{4V_S^2 V_{Sf}^2 (9V_S^2 + V_{Sf}^2)}{H^2[(6V_S^2 + V_{Sf}^2)^2 + 9V_S^4]} \tag{16}$$

where V_S and V_{Sf} are the shear wave velocities of the upper (retained) layer, and the foundation layer, respectively.

Two cases of wall geometry were examined ($B/H=0.4$ and 0.8), and two different values of the factor d_θ. Note that the two values of d_θ are obtained by changing the value of V_{Sf}, while keeping constant the value of V_S.

3.1.2. Static response

The heightwise distributions of the statically induced wall pressures $\sigma_{st}=\sigma_{st}(\eta)$ are shown in Fig. 18, for the examined values of d_θ and B/H. In the same graphs, the corresponding wall pressures resulting from the spring model are also plotted.

The recovery of the exact value of the stress at the heel of the wall was not possible due to numerical singularities in that area. However, these values will hardly affect the magnitude of the resultant horizontal force and of the overturning moment.

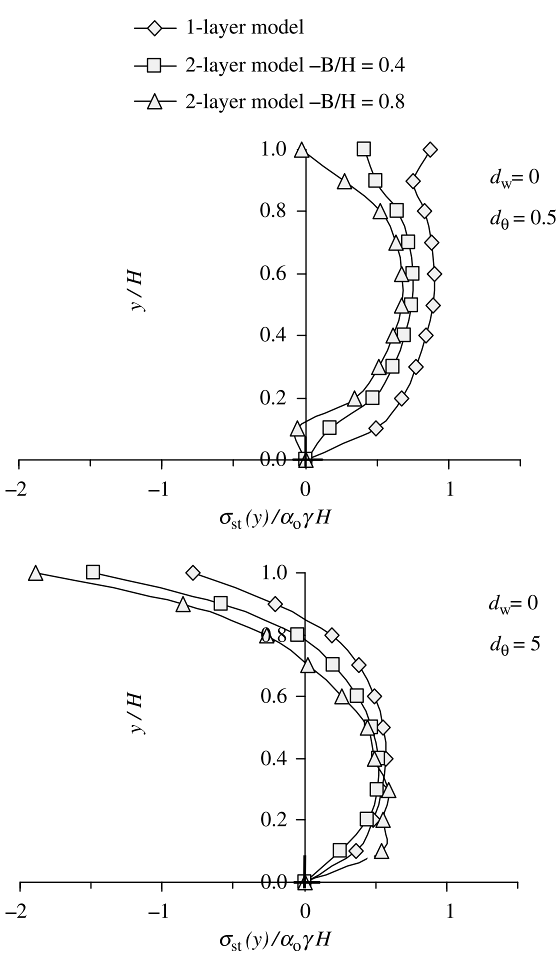

Fig. 18. Distribution of the quasi-statically induced wall pressures for the two-layer system and the equivalent single layer case.

It is observed that in general the increase in the degrees of freedom of the system leads to a decrease of the induced wall pressures. As it was already stated, the replacement of the Veletsos and Younan rotational spring at the base of the wall by an actual elastic soil layer introduces an additional degree of freedom to the system: the horizontal (transverse) elastic displacement of the wall. Consequently, the wall–soil system becomes more flexible, which, as anticipated, leads to a decrease in the wall pressures. Recall that this behaviour was previously observed in the case of flexible cantilever walls (see Figs. 4 and 5). Furthermore, the decrease in pressures is more noticeable when the B/H ratio attains relatively high values. This observation may be easily explained through the following example: consider two systems with identical soil profile geometry, and wall widths $B_1=B$ and $B_2=2B$. Notice from Eq. (13) that the rotational stiffness, K_r, is approximately proportional to the square of the wall width. This fact implies that for a given (constant) value of K_r, the stiffness of the soil supporting the wider wall has to be about a quarter of that supporting the narrower wall ($G_{f2}\approx G_{f1}/4$) for the rotational stiffness to remain the same. In turn, according to Eq. (14), the horizontal stiffness, K_h, is proportional to the stiffness of the underlying soil, G_f. Thus, the horizontal stiffness of the wider wall will be substantially lower than that of the narrower wall. For the particular cases examined herein, the horizontal stiffness of the wall with width $0.8H$ is about 30% of that of the wall with width $0.4H$. So, although the two systems have identical rotational stiffness (d_θ), the overall flexibility of the wall–soil system is higher in the case of $B=0.8H$, which is reflected on the resulting pressure distributions.

3.1.3. Harmonic response

The main two reasons, for which retaining walls with common rotational stiffness—but founded on different layers—will respond differently for the same excitation, were stated before. The effect of the horizontal translational stiffness K_h was seen through the study of statically excited systems. The impact of the underlying soil layer to the dynamic characteristics of the system is examined by considering a harmonic excitation in the special case of the two-layer profile resonance.

In Fig. 19, the heightwise wall pressure distributions are plotted for the examined values of d_θ and B/H. On the same graphs, the corresponding wall pressures resulting from the spring model are also plotted. Generally, the remarks made for the statically excited systems apply for the case of resonance as well. Furthermore, the dynamic texture of the excitation amplifies the discrepancies observed in the static case.

It is of great interest to examine the shear-base and the overturning-moment maximum dynamic amplification factors, which are given in Fig. 20 for the examined values of d_θ and B/H, and for the case of the spring model, as well. According to the spring model, the more flexible the wall–soil system is, the higher the dynamic amplification factors

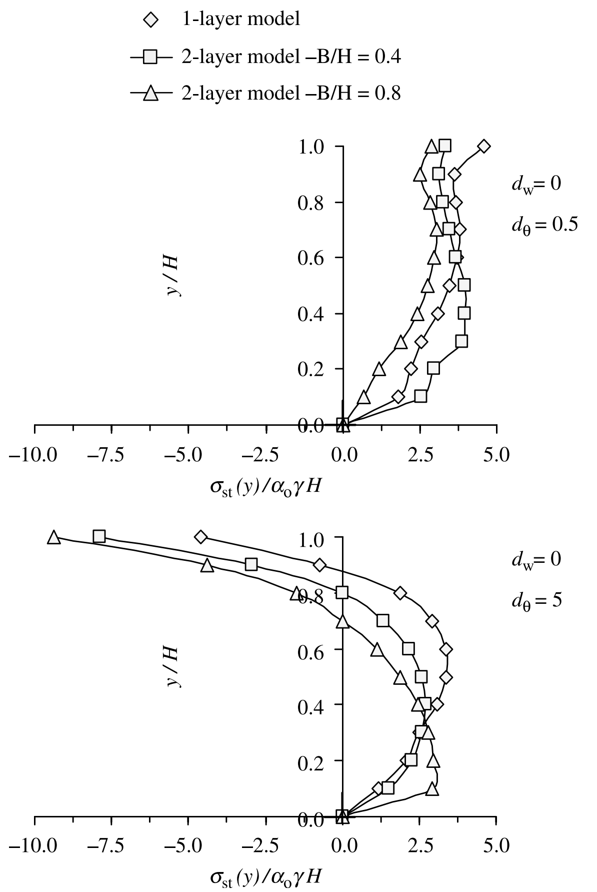

Fig. 19. Distribution of the wall pressures in the case of resonance ($\omega = \omega_1$): (a) $d_\theta = 0.5$, (b) $d_\theta = 5$.

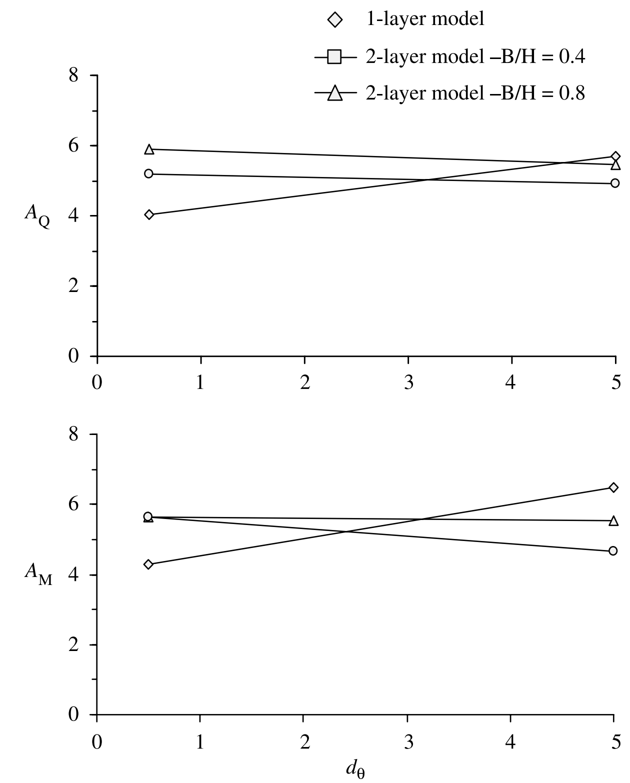

Fig. 20. Maximum dynamic amplification factors A_Q and A_M for the resultant horizontal force and the resultant overturning moment, respectively, in the case of resonance ($\omega = \omega_1$).

are. The consideration of a more realistic model, as the one adopted in this study, leads to the opposite conclusion. The discrepancy between the two approaches can be justified as follows: In the spring model the stiffness of the rotational constraint is real-valued, and therefore, the damping capacity of the wall itself cannot be taken into consideration. As a consequence, the impinging waves on the wall cannot be dissipated, while the rotational oscillation of the wall increases the wave amplitude. So, in the spring model, the increase in the wall base flexibility leads to higher values of the dynamic amplification factors. On the contrary, at the present approach the rotation of the wall is governed by not only the rotational stiffness, but the damping characteristics (radiation and material damping) of the foundation layer, as well. In this way, the wave energy can be dissipated by the boundaries of both the retained and the underlying soil. Additionally, higher values of impedance contrast α ($= V_S/V_{Sf}$ in the case of common density) cause larger wave dissipation, and consequently, smaller dynamic amplification. It is noted that quite recently Li [9,10] extended the results of Veletsos and Younan by analysing the dynamic response of gravity walls founded on homogeneous elastic half-space. Thus, in addition to rotational stiffness, they accounted for rotational damping (due to radiation and hysterysis), and came up with conclusions similar to those of our study.

4. Conclusions

The paper utilizes the finite-element method to study the dynamic earth pressures developed on rigid or flexible non-sliding retaining walls. Modelling the soil as a visco-elastic continuum, the numerical results are shown to converge to the analytical solutions of Wood [24] for a rigid fixed-base wall and of Veletsos and Younan [23] for a wall that has structural flexibility or rotational flexibility at its base, and retains a single-soil layer.

The method is then employed to further investigate parametrically the effects of flexural wall rigidity and base compliance in rocking. Both homogeneous and inhomogeneous retained soil layers are considered, while a second soil layer is introduced as the foundation of the retaining system. The results confirm the crude convergence between Mononobe–Okabe and elasticity-based solutions for structurally or rotationally flexible walls. At the same time they show the beneficial effect of soil inhomogeneity. Wave propagation in the underlying foundation layer may have an effect that cannot be simply accounted for with an appropriate rocking spring at the base.

One of the limitations of both the analytical solution of Veletsos and Younan [23] and the numerical model of this paper stems from the assumed complete bonding in the wall–soil interface. This can be rather inaccurate in the case of flexible systems, due to the development of unrealistic tensile stresses at the interface especially near the ground surface. It was observed, however, that such tensile stresses diminish in the case of inhomogeneous retained soil, which our model examined.

References

[1] Al-Homoud AS, Whitman RV. Comparison between fe prediction and results from dynamic centrifuge tests on tilting gravity walls. Soil Dyn Earthquake Eng 1994;14:259–68.

[2] Al-Homoud AS, Whitman RV. Seismic analysis and design of rigid bridge abutments considering rotation and sliding incorporating non-linear soil behaviour. Soil Dyn Earthquake Eng 1999;18: 247–77.

[3] Arias A, Sanchez-Sesma FJ, Ovando-Shelley E. A simplified elastic model for seismic analysis of earth-retaining structures with limited displacements. Proceedings of the international conference on recent advances in geotechnical earthquake engineering and soil dynamics, vol. 1. St Louis, MO; 1981. p. 235–40.

[4] Biggs JM. Introduction to structural dynamics. New York: McGraw-Hill; 1964.

[5] Dobry R, Gazetas G. Dynamic response of arbitrarily shaped foundations. J Geotech Eng Div, ASCE 1986;112(GT2):109–35.

[6] Gazetas G. Foundation vibrations. In: Fang HY, editor. Foundation engineering handbook. 2nd ed. New York: Van Nostrand Reinhold; 1991. p. 553–93 [chapter 15].

[7] Gazetas G, Psarropoulos PN, Anastasopoulos I, Gerolymos N. Seismic behaviour of flexible retaining systems subjected to short-duration moderately-strong excitation. Soil Dyn Earthquake Eng 2004;24:537–50.

[8] Hibbit, Karlsson & Sorensen, Inc. ABAQUS Code; 1998.

[9] Li X. Dynamic analysis of rigid walls considering flexible foundation. J Geotech Geoenviron Eng, ASCE 1999;125(9).

[10] Li X, Aquilar O. Elastic earth pressures on rigid walls under earthquake loading. J Earthquake Eng 2000;4(4):415–35.

[11] Mononobe N, Matsuo H. On the determination of earth pressures during earthquakes. Proceedings of the world engineering congress, Tokyo, Japan. vol. 9 1929 paper no. 388.

[12] Nadim F, Whitman RV. Seismically induced movement of retaining walls. J Geotech Eng, ASCE 1983;109(7).

[13] Newmark NM. Effects of earthquakes on embankments and dams. Géotechnique 1965;15(2):139–60.

[14] Okabe S. General theory of earth pressures. J Jpn Soc Civil Eng 1926; 12(1).

[15] Psarropoulos PN, Klonaris G, Gazetas G. Seismic response of retaining walls. Proceedings of the fourth Greek conference of geotechnical and geo-environmental engineering, Athens. vol. 2 2001 p. 377–85.

[16] Regulatory Guide E39/93 for the seismic analysis of bridges (Ministry of Public Works). Bulletin of Greek Technical Chamber; 1998, No. 2040.

[17] Richards R, Elms DG. Seismic behavior of gravity retaining walls. J Geotech Eng Div, ASCE 1979;105:449–64.

[18] Scott RF. Earthquake-induced pressures on retaining walls. Proceedings of the fifth world conference on earthquake engineering. vol. 2 1973 p. 1611–20.

[19] Seed HB, Whitman RV. Design of earth retaining structures for dynamic loads. Proceedings of the special conference on lateral stresses in the ground and design of earth retaining structures 1970 p. 103–47.

[20] Travasarou Th, Gazetas G. On the linear seismic response of soils with modulus varying as a power of depth—the maliakos marine clay. Soils Found 2004;44(5):85–93.

[21] Veletsos AS, Younan AH. Dynamic soil pressures on rigid vertical walls. Earthquake engineering and structural dynamics. vol. 23. New York: Willey; 1994 p. 275–301.

[22] Veletsos AS, Younan AH. Dynamic modeling and response of soil-wall systems. J Geotech Eng, ASCE 1994;120(12):2155–79.

[23] Veletsos AS, Younan AH. Dynamic response of cantilever retaining walls. J Geotech Geoenviron Eng, ASCE 1997;123(2): 161–72.

[24] Wood JH. Earthquake–induced pressures on a rigid wall structure. Bull New Zealand Natl Earthquake Eng 1975;8:175–86.

[25] Roesset JM. Soil amplification of earthquakes. In: Desai CS, Christian JT, editors. Numerical methods in geotechnical engineering, 1977. p. 639–82 [chapter 19].

[26] Kramer S. Geotechnical earthquake engineering. NJ, USA: Prentice Hall; 1996.